Fall 12-2013

RNA interference targeting Glucose-Regulated-Protein 78 induces HepG2 cell Apoptosis

Brittany Blackman
brittany.blackman@student.shu.edu

RNA interference targeting Glucose-Regulated-Protein 78 induces HepG2 cell Apoptosis

By

Brittany Alexandra Blackman

A Thesis

Submitted in partial fulfillment of the requirements for the

degree of Master of Science in Biology

in

Department of Biological Sciences of Seton Hall University

December 2013

APPROVED BY

_____

MENTOR

Dr. Allan Blake

_____

COMMITTEE MEMBER

Dr. Constantine Bitsaktsis

_____

COMMITTEE MEMBER

Dr. David Sabatino

_____

DIRECTOR OF GRADUATE STUDIES

Dr. Allan Blake

_____

CHAIR, BIOLOGICAL SCIENCES DEPARTMENT

Dr. Jane Ko

ACKNOWLEDGEMENTS

I would like to express my appreciation to the following people:

Dr. Allan Blake, my mentor, for giving me the opportunity to develop as a research scientist in his lab, and for his excellent tutelage and guidance in my education and career.

Dr. David Sabatino, my co-mentor, for his patience and guidance in the area of biochemistry.

Dr. Constantine Bitsaktsis, for his willingness to be a member of my thesis committee and his help with the completion of my degree.

Dr. Jane Ko, the departmental chair, for allowing me to perform research in Seton Hall's Biological Sciences Department.

Jeanette Walton for her guidance and support as a laboratory mate throughout my time at Seton Hall University.

The Biology Department faculty and staff for their continued support throughout my endeavors.

Seton Hall University for providing me with the opportunity to pursue my post-graduate education.

TABLE OF CONTENTS

FIGURES

TABLES

ABSTRACT

Cancer is a complex genetic disease that is driven by genetic mutations resulting in chronic, inappropriate cell proliferation. Many current cancer therapies lack specificity towards tumor tissues, ultimately leading to adverse side effects and limited clinical efficacy. Recently, selective cancer cell therapy has examined a well-characterized cell surface marker that is preferentially expressed on tumor cells. The over-expression of an endoplasmic reticulum chaperone protein, 78-kDa glucose-regulated-protein (GRP78), has been observed on the surface of cancer cells, but not on normal tissues. By selectively targeting GRP78 with short-interfering RNA (siRNA), potent GRP78 silencing is anticipated by the RNA interference (RNAi) pathway. Silencing GRP78 expression is expected to compromise cell signaling activity, ultimately resulting in cancer cell death. Towards this effect, I have shown that linear, branched and hyper-branched GRP78-targeting siRNA constructs elicited significant reductions in GRP78 protein expression (40 – 60%) in a cell culture model of human liver cancer, the HepG2 cell. The siRNA-hyper-branched A-1-2 construct produced 18% more knockdown when compared to its linear siRNA controls (siRNA-GRP78-1 + GRP78-2). This result highlights the synergistic effects of the novel A-1-2 construct, which combines two different GRP78-targeting siRNA motifs within a single molecular structure. A greater reduction in GRP78 expression resulted in greater apoptotic cell death. The novel siRNA motifs, specifically V-branched and A-1-2 hyper-branched, elicited the most cell death, 11 -12%, revealing that they may enhance cell apoptosis by conferring stable and potent siRNA structures. Effectively targeting cell surface GRP78 with siRNA provides a selective approach for compromising human cancer cell activity.

INTRODUCTION

Cancer is defined as a complex genetic disease caused by a mutation of tumor suppressor genes or oncogenes; specifically due to an alternation of signaling pathways and has multiple links to programmed cell death (Ouyang et al., 2012). In a recent comprehensive cancer biology survey, Dr. Robert Weinberg identifies six features of cancer: sustaining proliferative signaling, evading growth suppressors, activating invasion and metastasis, enabling replicative immortality, inducing angiogenesis and resisting cell death (Hanahan and Weinberg, 2011). Cancer cells are able to sustain chronic proliferation by deregulating the cell cycle to promote cell growth. Two important regulators of the cell cycle are pRB (retinoblastoma protein) and Tp53, tumor suppressor proteins that receive signals that can inhibit cell cycle progression and trigger apoptosis (Hanahan and Weinberg, 2011). pRB integrates growth-inhibitory signals from diverse extracellular and intracellular sources which dictates whether a cell should proceed through a regulated cell cycle. Tp53 activates apoptosis by up-regulating the pro-apoptotic BH3 proteins Noxa and Puma in response to substantial chromosomal abnormalities and DNA breaks (Hanahan and Weinberg, 2011).

Two other hallmarks of cancer pathogenesis include the ability to modify and reprogram cellular metabolism to support their proliferation and evasion of immunological destruction by T and B lymphocytes, macrophages and natural killer cells (Grivennikov et al., 2010; Hananhan and Weinberg, 2011). Pro-inflammatory responses by innate immune cells can result in tumor progression (Hanahan and Weinberg 2011). Additionally, genomic mutations allow cancer cells with genetic alterations to drive tumor progression. Certain oncogenes such as *ras* and *myc* induce transcription that can lead to remodeling of tumor microenvironment. Recruitment of

leukocytes or lymphocytes that express tumor promoting cytokines or chemokines can lead to the induction of angiogenesis (Grivennikov et al., 2010). Once tumors are oxygen and nutrient deprived, necrotic cell death occurs at the tumor's core causing the release of pro-inflammatory mediators: IL-1 (interleukin-1) and HMGB1 (High Mobility Group Box 1) (Grivennikov et al., 2010).

Inflammatory and innate cells provide cancer cells with additional growth factors to promote survival. Immune cells communicate with each other either by direct contact or indirectly by the production of cytokines and chemokines in an autocrine or paracrine manner to control tumor growth (Grivennikov et al., 2010). Expression of various immune mediators and the activation state of different cell types in the tumor microenvironment dictates whether inflammation promotes tumor growth or anti-tumor immunity. TAMS (tumor associated macrophages) and T regulatory cells promote tumor growth and may be necessary for angiogenesis, invasion and metastatsis (Grivennikov et al., 2010). Different cytokines can promote or inhibit tumor development and progression. IL-6, IL-17, IL-23 enhances tumor progression while IL-12 and IFN-gamma inhibit tumor progression (Grivennikov et al., 2010). IFN-gamma activates macrophages to express pro-inflammatory cytokines (TNF-alpha, IL-12) to prime anti-tumor immune responses. TNF (Tumor Necrosis Factor) and Fas-L once bound to their receptors stop tumor progression by causing tumor cell death (Grivennikov et al., 2010).

Apoptosis is a major type of programmed cell death that occurs when DNA damage is irreparable (Ouyang et al., 2012). Impaired apoptosis is frequently associated with hyper-proliferative conditions such as cancer (Kepp et al., 2012). Two core pathways that induce apoptosis are the extrinsic death receptor pathway and the intrinsic mitochondrial pathway.

Death receptor pathway is triggered by binding of Fas receptor with Fas-L (extracellular ligand) to form a death complex, FADD (Fas Associated Death Domain). FADD activates pro-caspase 2/pro-caspase 8; followed by caspase 6 which triggers the conversion of pro-caspase 3 into activated caspase 3/caspase 7 to execute apoptosis (Ouyang et al., 2012). TNF (Tumor-Necrosis-Factor) can bind to TNF-Receptor to activate FADD and result in programmed necrosis (Ouyang et al., 2012). In the mitochondrial pathway, the mitochondrial enzymes initiate the apoptotic process. The outer mitochondrial membrane becomes permeable to cytochrome *c* being released from the mitochondria into the cytosol. Pro-caspase 9 is activated and forms a protein complex with APAF-1, to become the apoptosome, activating caspase 3/caspase 7 ending in apoptosis (Ouyang et al., 2012). Apoptosis is regulated by the balance of the anti-apoptotic protein (Bcl-2) and the pro-apoptotic protein (Bax). Bcl-2 inhibits apoptosis by suppressing Bax. Tumors are able to evade apoptosis by increasing the expression of anti-apoptotic regulators (Bcl-2) or survival signals (Igf ½) and down-regulating pro-apoptotic factors such as Bax and Bim (Hanahan and Weinberg, 2011).

Accumulating evidence has demonstrated that abnormal expression in key regulatory factors may lead to cancer (Hanahan and Weinberg, 2011). The cellular antiapoptotic machinery is composed of upstream regulators that process extracellular death inducing signals (Fas/Fas ligand receptor and intracellular signals) and downstream effector components (caspase 8 and caspase 9). An apoptotic trigger conveys signals between the regulators and effectors. Apoptosis is controlled by counterbalancing the pro-apoptotic and anti-apoptotic Bcl-2 regulatory proteins that are over-expressed in many cancer cells (Hanahan and Weinberg, 2011). Specifically, reduced Bcl-2 (Bcl-2 and Bcl-XL) expression promotes apoptotic responses to chemotherapeutic

drugs while increased Bcl-2 expression promotes resistance to chemotherapeutic drugs and radiation therapy (Ouyang et al., 2012).

Necrosis is a random, uncontrolled process of cell death when compared to apoptosis. Necrosis has the potential to be pro-inflammatory and promote the progression of tumors (Galluzzi et al., 2009). Necrotic cells release their intracellular contents into the surrounding microenvironment (Hanahan and Weinberg, 2011). The key mediators in necrosis are RIP (Receptor interacting protein) kinases, PARP (poly ADP-ribose polymerase), and NADPH oxidases (Ouyang et al., 2012). Necrotic cell death stresses can activate PARP, inducing necrosis through the activation of RIP kinases (RIP1 and RIP3). RIP kinases influence the mitochondria directly while NADPH oxidase influences the mitochondria indirectly by inducing an increase of ROS (reactive oxygen species) leading to necrotic cell death (Ouyang et al., 2012). The membranes of cells that undergo necrosis become disrupted. Once disrupted, the intracellular components are released into the extracellular leading to inflammatory responses by immune cells. Local inflammation that is induced by programmed necrosis may serve to promote tumor growth (Ouyang et al., 2012). Necrotic cells release pro-inflammatory signals which recruit immune cells. Although phagocytosis aids in removing necrotic cellular debris, inflammatory cell chemicals, such as reactive oxygen species, are also released. The highly mutagenic ROS release can impact neighboring cells thereby accelerating the malignant process (Hanahan and Weinberg, 2011; Grivennikov et al., 2010).

A significant limitation of current cancer therapies is a lack of specificity towards tumor tissues, which ultimately can lead to adverse side effects limiting their clinical efficacy (Liu et al., 2007). Delivering anticancer drugs specifically to the target tumor cells could potentially

reduce unwanted non-specific toxicity. Recently, progress towards the goal of targeted therapy delivery has been explored by the characterization of a cell surface marker that is preferentially expressed on tumor cells (Wang et al., 2009). The over-expression of 78-kDa glucose-regulated-protein (GRP78), also known as Bip or HSPA5, has been reported on the surface of cancer cells (Wang et al., 2009) and has facilitated the selective internalization of potent anti-cancer drugs in metastatic melanoma tissues and in xenograft mouse models (Kim et al., 2006; Liu et al., 2007; Yoneda et al., 2008). Therefore, GRP78 functions as a relevant molecular marker for the development of selective anti-cancer strategies.

GRP78 is an intracellular endoplasmic reticulum (ER) chaperone and a member of the heat shock protein 70 (HSP70) family that normally provides a protective response against cellular stress conditions. ER chaperones are required for normal function of protein folding. GRP78 is specifically involved in the translocation of newly synthesized polypeptides across the ER membrane, targeting mis-folded proteins for ER-associated degradation (ERAD), buffering Ca^{2+} levels and serving as a ER stress sensor (Wang et al., 2009).

GRP78 controls activation of the unfolded protein response (UPR), as well as associated apoptotic pathways (Wang et al., 2009). In the unstressed cell, intracellular GRP78 is bound to ER-transmembrane signaling molecules and ER-associated pro-caspase 12 (Wang et al., 2009). After ER stress induction, GRP78 dissociates from the ATF6 (Activating Transcription Factor 6), IRE1 (Inositol-Requiring Enzyme 1) and PERK (PKR-like ER kinase) stress transducers, thereby activating either the survival pathway to prevent further cellular damage or apoptosis if the damage is irreparable (Wang et al., 2009). Next, the pro-apoptotic Bax protein in the ER membrane undergoes conformational change to allow Ca^{2+} to enter the cytosol. M-calpain is

cleaved activating pro-caspase 12 to further activate the caspase cascade (via activation of caspase 9 and caspase 3/caspase 7). Cellular hypoxia and glucose deprivation that occur in the tumor microenvironment activate the ER UPR which in turn up-regulates GRP78 transcription (Wang et al., 2009). While an increase in stress-induced GRP78 transcription correlates with increased cell survival, it has been reported that this over-expression results in GRP78 cell surface localization. It is noteworthy that cell surface GRP78 expression has been detected on highly metastatic prostate cancer cells where it may mediate signal transduction pathways that promote proliferation (Lee, 2007).

GRP78 expression levels are substantially elevated in primary tumors of breast cancer, lung cancer, prostate cancer and hepatocellular carcinoma (Wang et al., 2009). Hepatocellular carcinoma is the most common primary cancer of the liver, with a significant increase in the incidence in the United States over the past 20 years (El-Serag and Mason, 1999). The HepG2 cell line was derived from a biopsy of a liver cancer patient (Javitt, 1990). The HepG2 cell line shows distinctive developmental characteristics of a hepatoblastoma, an early developmental malignancy of childhood (Javitt, 1990). The metabolic processes that have been studied with the HepG2 cell line indicate it is a useful model of human liver cancer (Javitt, 1990).

RNA interference (RNAi) is a cellular mechanism for controlling gene expression where siRNAs are bound to an RNA-induced silencing complex (RISC) to mediate mRNA cleavage and degradation through catalytic process involving endonucleases (Taberno et al., 2013). RNAi can target any gene in the human genome using small interfering RNAs (siRNA) or micro RNAs (miRNAs). *Dicer* and *Argonaute* (*Ago*) are important ribonucleases in the RNAi mechanism. RNAi operates in a Dicer-dependent manner or by posttranscriptional mechanisms. RNAi

mechanism begins with the conversion of dsRNA (double stranded RNA) into small RNAs (siRNA) by Dicer an RNase III nuclease (Paddison et al., 2002). The small RNAs are incorporated within a protein complex (RISC) using the sequence of siRNAs to identify and destroy homologous mRNAs (Paddison et al., 2002; Bernstein et al., 2001). Ago proteins are components of the RISC complex that once activated targets, cleaves and degrades the mRNA.

Small interfering RNAs are synthesized products of Dicer and function as the biologically active structures in the RNAi pathway (Paddison et al., 2002). The chemically synthesized siRNAs can bypass the requirement for Dicer and enter the silencing pathway by incorporating into the RISC complex. Moreover, they may incorporate modified nucleic acids or structural motifs that improve stability and gene silencing efficacy for therapeutic applications (Bumcrot et al., 2006). siRNAs and vectors containing dsRNA triggers can be transiently transfected into mammalian cells using different transfection reagants (Paddison et al., 2002). Systemic delivery of siRNAs is required for widest application of RNAi therapeutics (Taberno et al., 2013).

The presence of the RNAi pathway for regulating gene expression in all mammalian cell types forms the basis of our targeted anti-cancer approach. Since GRP78 is only found on the cell surface of tumors, it is possible to target cell surface GRP78 function, using it as a cancer-targeting marker for potential therapeutic applications (Lee, 2007). In our current study, we examine the effects of RNA interference using multiple siRNA constructs specific to GRP78 to explore GRP78's role in apoptosis of HepG2 cancer cells.

MATERIALS AND METHODS

HepG2 cell culture

The human hepatocyte cell line, HepG2 cells (American Type Culture Collection, Manhasset, VA) was propagated in monolayer culture as described (Maina et al., 2013). HepG2 cells were maintained in T25 cm^2 and T75 cm^2 flasks (Grenior Bio-one Cell star, FL) in Dulbecco's Modified Eagle Medium (DMEM) with GlutaMAX and heat-inactivated 10% Fetal Bovine Serum (Invitrogen, CA), containing 1% penicillin/streptomycin (Invitrogen, CA), in a humidified atmosphere with 5% CO2. All the solutions were certified cell culture grade (Invitrogen, CA). Cells were routinely passaged at 75% confluence using Dulbecco's PBS (Invitrogen, CA) for rinsing and 0.05% Trypsin-EDTA (1X), Phenol Red (Invitrogen, CA) and split 1:10 (dish:dish ratio). Cells used in experiments were cultured in 6-well, 12-well, 24-well or 96-well culture plates and were allowed to recover for 24 hours before treatment.

Preliminary Assays

Experimental optimization studies were conducted prior to starting the actual transfection experiments. This included determining the optimal plating cell density, the amount of transfecting reagent (Lipofectamine 2000; Invitrogen, CA) and the experimental oligonucleotides (Dr. Sabatino's Lab; Seton Hall University, NJ) to be used in the protocol. For testing Lipofectamine toxicity, cells were plated at 50,000 cells/well in a 96 well plate and increasing amounts of Lipofectamine 2000 were added to each well (0.5 to 10.0 µl/well). After 48 hours, cell viability was determined with 1 mg/ml of Calcein AM (in Opti-MEM; Invitrogen, CA) added to each well and the plate was returned to the growth incubator for 20 minutes. The cells were then washed with PBS and cell-retained fluorescence was determined in a Cytoflour 4000 fluorescence plate reader (Applied Biosystem, CA) with an excitation at 450 nm and emission at 530 nm. For the cell density experiment, HepG2 cells were plated at 30,000, 40,000, 50,000, 60,000, 70,000 and 80,000 cells/well, with and without Lipofectamine (1 µl/well) treatment in 24 well plates. After 48 hours, just as in the other preliminary experiment, cellular Calcein AM was used to assess toxicity, as described above. Cell fluorescence data were transferred from the Cytofluor 4000 software to GraphPad Prism 5.0 (GraphPad, CA) for analysis. Data presented are expressed as the mean +/- S.E.M., with $p < 0.05$ defined as significant.

siRNA Transfection

HepG2 cells were transfected with Lipofectamine 2000 (Invitrogen Life Technologies, CA), as described above ("Preliminary Assays"). Twenty four well plates were used, each containing 5 x 10^4 cells/well in DMEM with 10% fetal bovine serum and maintained for 48 h in a humidified incubator at 37°C with 5% CO_2. Twenty four hours prior to transfection the cells were washed twice with PBS and switched to a basal, serum free medium (Opti-MEM). Transfections were performed with 1 µl Lipofectamine 2000 and 50 µl of the appropriate siRNA dilution (40 pmol siRNA in Opti-MEM) using, sterile filtered pipet tips (Molecular Bioproducts Fisher Scientific, CA). The siRNA-Lipofectamine complexes were incubated at room temperature for 20 min, then 100 µl of appropriate solution was added to the cell monolayers and the plates were incubated at 37°C with 5% CO_2. After 24 hours, the serum free basal medium was removed and replaced with growth medium containing 10% FBS. Transfected cells were harvested 48 hours after transfection for analysis.

The experimental siRNA oligonucleotides used in the transfection experiments were synthesized and provided by Dr. Sabatino's lab (Seton Hall University, NJ).

Cell Viability Trypan Blue Exclusion Assay

Cell viability assays were performed in 24-well plates in serum-free basal medium (Opti-MEM) for 24 hours and then incubated in the presence or absence of appropriate treatment for 24 hours at 37^{o}C. Following incubation for 24 hours, the treatment solution was removed and the cells were placed in DMEM with 10% FBS. After treatment for 24 hours, the samples were removed with Enzyme Free Dissociation Buffer (Invitrogen, CA) for 3 minutes at 37°C. Samples were then pelleted by microcentrifugation (500 rpm at room temperature) and resuspended in 1 mL of PBS and 100 µL of Trypan Blue 0.4% stain (Invitrogen, CA) was added. An aliquot (12 µl) was then quantified using a Countess automated cell counter (Invitrogen, CA). The resulting data was analyzed with GraphPad Prism 5.0 and statistical significance was determined by ANOVA ($p < 0.05$).

Cell Lysis and Protein Assay

Cell lysates were prepared using a sterile RIPA Lysis Buffer (TekNova, CA) with 1:1000 Protease Inhibitor Cocktail mix (cOmplete ULTRA Tablets, mini, EASYpack, Roche, NJ). Protease Inhibitor tablets were dissolved in 5 ml of sterile deionized water, stored in -20°C for 4 weeks. Thawed inhibitor cocktail was added to the RIPA lysis buffer at 100 ul/well on a 24 well plate. Plates were then placed on ice for 10 – 15 minutes before cells were transferred to labeled 1.5 ml centrifuge tubes and spun at 14,000 rpm for 10 minutes in 4°C. Cell supernatants were removed, placed into new tubes and stored in -80°C prior to using them in a protein assay for protein concentration determination, SDS-PAGE and Western blot analysis (Invitrogen, CA).

Protein concentration was determined using a Protein Assay Kit (Thermo Pierce, IL) according to the manufacturer's instructions. Briefly, 2 mg/ml Albumin solution was used as a standard for generating a standard calibration curve. The 2 mg/ml solution was diluted in PBS (Invitrogen, CA) to create standard solutions using serial dilutions. HepG2 protein samples were diluted in 1:10 (v/v) solution of PBS and placed on shaker for 5 minutes. A solution of BCA reagent (A: bicinchoninic acid) is added to solution B (B: Copper ionic solution; 50:1, v/v). Protein sample (25 µL) was added to a single well of 96 well plate in duplicate and then 200 µl of BCA reagent (A and B mixed together) was added on top of the protein sample. The plate was wrapped in plastic wrap and placed in 37°C water bath for 35 minutes before being read on Spectramax 250 (Molecular Devices, CA) at 562 nm to establish a concentration-dependent calibration curve. Sample protein concentrations were then determined from the calibration curve.

Western Blot

Parallel cultures of HepG2 cells were prepared with serum-free basal medium (Opti-MEM) for 24 hours and then incubated in the presence or absence of the appropriate siRNA (40 pmol) for 48 hours at 37˚C. Cellular protein lysates were prepared with RIPA lysis buffer and mixed with NuPAGE LDS Sample Buffer 4X (Invitrogen, CA) then heated to 70˚C for 10 min., resolved on NuPAGE Novex 10% Bis-Tris Gel 1.0 mm, 12 well (Invitrogen, CA) at 150 volts using the XCell SureLock Mini-cell system, (Invitrogen, CA) for 1 hour and electroblotted onto polyvinyldifluoride (PVDF) membranes (Biorad, CA). The PVDF membrane was treated for 90 min in a blocking buffer containing 5% (w/v) of non-fat dehydrated milk in TBS (0.1% Tween 20; Biorad, CA). GRP78 expression was immunodetected with a 1:200 dilution of anti-GRP78 N-20 antibodies (Santa Cruz Biotechnology, CA) in 2.5% non-fat dehydrated milk in TBST. The membrane associated immunoreactivity was then detected using a 1:5000 dilution of a horseradish peroxidase-conjugated anti-goat secondary antibody and detected using ECL Plus chemiluminescence (GE Amersham Life Sciences, NJ). The resulting autoradiograph was scanned with Storm 860 Phosphoimager Electrophoresis Scanner (GE Amersham Molecular Devices, NJ), quantified with NIH ImageJ and expressed as integrated pixel density, as previously described (Badway et al., 2004).

Confocal Microscopy

HepG2 cells were plated at a cell density of 1.5 x 10^5 cells/well on 4 well chamber glass slides (Nunc Lab Tek Thermo Scientific, NJ) and were treated after 48 hours. Post treatment (24 hours), cells were rinsed with serum free DMEM then fixed with 2% paraformaldehyde in PBS (Invitrogen, CA) for 10 minutes. Slides were then blocked in 10% rabbit serum (Invitrogen, CA) in PBS and placed on a shaker for 30 minutes, then incubated in goat-anti human GRP78 N-20 antibody (Santa Cruz Biotechnology, CA) 1:75 dilution in 2.5% rabbit serum in PBS for 2 hours at room temperature. After PBS washing the slides were incubated in goat anti-rabbit conjugated with fluorescin (FITC) antibody (Vectashield, Vector Laboratories, CA) in 2.5% rabbit serum in PBS for 50 minutes covered to protect from photobleaching. Slides were counterstained with DAPI in 0.5 ug/mL in PBS for 3 minutes then a mounting medium (Vectashield, Vector Laboratories, CA) with fluorescence was added with coverslips. Slides were viewed on Confocal Laser Scanning Microscope with 40X oil objective lens in conjunction with the Olympusview 3.1 program.

Statistical Analysis

All the results from the different data groups were calculated and presented as the mean +/- S.E.M. for each control or treatment. Statistical comparisons between the means of different groups were performed by ANOVA with Tukey multiple comparison post-test. Data was analyzed using GraphPad Prism 5.0 and statistical significance defined as $P < 0.05$.

RESULTS

Preliminary Experiments and Lipofectamine Toxicity

Figure 1 displays the optimization experiments conducted prior to the siRNA transfections within HepG2 cells. Prior to transfection, a Western blot was used to detect the total amount of GRP78 in HepG2 cells (Fig1C). Two different types of lysis buffers; RIPA Lysis Buffer and LDS NuPAGE were used. HepG2 cells were grown on 6 well plates and lysed with two different buffers. RIPA lysis buffer produced sharper bands than the NuPAGE LDS buffer; a main band at 78 kDa for GRP78 expression was detected for both samples. Multiple bands were detected due to nonspecific binding to the secondary antibody used in the experiment. To remove the nonspecific binding a different secondary antibody was used in future Western blot experiments.

In order to determine Lipofectamine toxicity within HepG2 cells, increasing amounts of Lipofectamine 2000 (from 1 µg/well to 10 µg/well) was administered to cells in a 96-well plate (9 wells/treatment). Calcien AM cell viability assay was administered 48 hours post treatment (Fig1A). Only cells treated with 10 µg of Lipofectamine showed any significant drop in cell viability 48 hours post treatment (Fig1A). Optimization for the correct plating density to be used for siRNA transfection was determined by growing cells at increasing plating densities (from 30,000 cells/well to 80,000 cells/well) in 24 well plate (4 wells/treatment) with and without 1 ug/well treatment of Lipofectamine 2000 (Fig1B). Forty-eight hours post treatment Calcain AM cell viability assay was administered. Based on the viability results, 50,000 cells/well were chosen to be used for RNAi transfection experiments.

A.

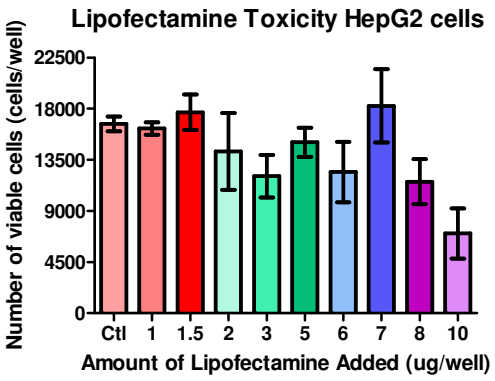
Lipofectamine Toxicity HepG2 cells
Number of viable cells (cells/well)
22500
18000
13500
9000
4500
0
Ctl 1 1.5 2 3 5 6 7 8 10
Amount of Lipofectamine Added (ug/well)

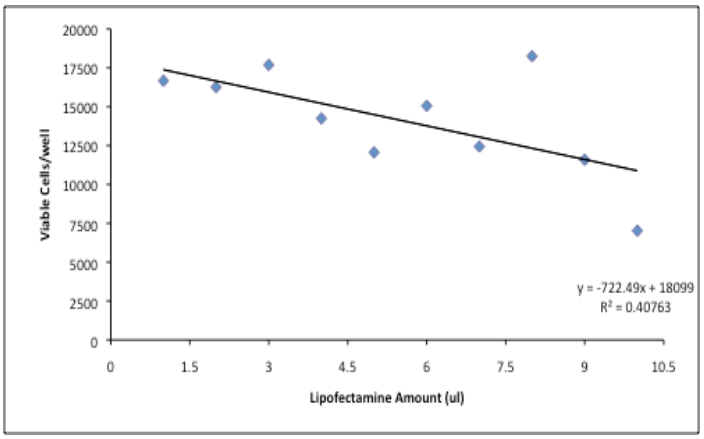
Viable Cells/well
20000
17500
15000
12500
10000
7500
5000
2500
0
0 1.5 3 4.5 6 7.5 9 10.5
Lipofectamine Amount (ul)
y = -722.49x + 18099
R² = 0.40763

B.

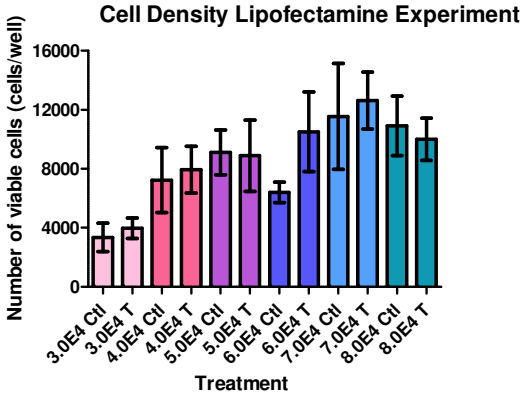
Cell Density Lipofectamine Experiment
Number of viable cells (cells/well)
16000
12000
8000
4000
0
3.0E4 Ctl
3.0E4 T
4.0E4 Ctl
4.0E4 T
5.0E4 Ctl
5.0E4 T
6.0E4 Ctl
6.0E4 T
7.0E4 Ctl
7.0E4 T
8.0E4 Ctl
8.0E4 T
Treatment

C.

D.

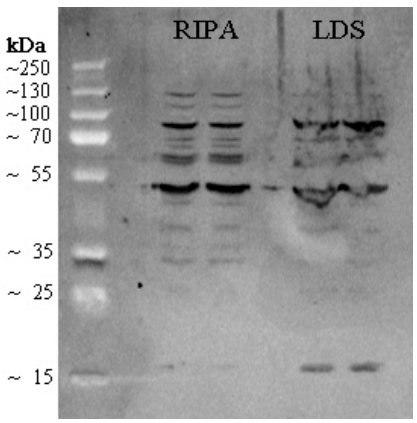

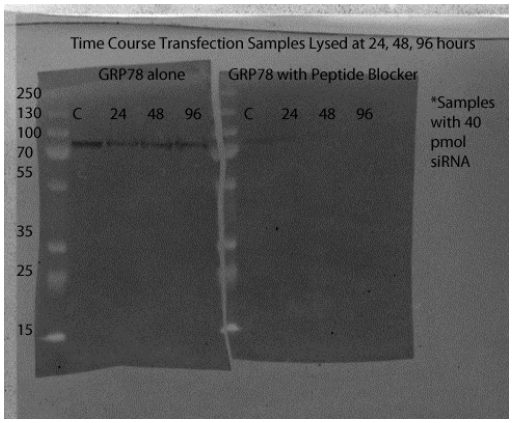

Figure 1: Preliminary experiments and Lipofectamine toxicity testing, **A.** HepG2 cells were plated 50,000 cells/well in 96 well plate with 9 wells per treatment. The number of viable cells/well after Calcien AM treatment is shown (n=1). **B.** Increasing cell plating densities with and without 1 µg Lipofectamine/well in a 24 well plate (From 30,000 cells/well to 80,000 cells/well (4 wells/per treatment; n=1). **C.** Western blot detection of GRP78 using the lysis buffers, primary anti-GRP78 and a HRP-conjugated second antibody. Cells grown on a 6 well plate were lysed with the lysis buffers RIPA (left duplicate lanes 1 & 2) and LDS (right duplicate lanes 3& 4). Twenty micrograms of HepG2 protein was loaded per lane. Experiment n=1. **D.** HepG2 western blot of 15 ug of cell lysate prepared from a post-transfection time course with 40 pmol of siRNA GRP78-1 at 24 h, 48h and 96 h. Fifteen micrograms of HepG2 total protein s were loaded per lane to detect GRP78 protein levels by western blotting with a GRP-78 polyclonal antibody. A peptide specific to the immunogen region of GRP78 was used on identical samples on the right to demonstrate that the band present is GRP78 protein expression. Experiment n=1.

RNAi Optimization

The optimal concentration of siRNA to be used for RNAi transfection experiments was established with increasing amounts of siRNA GRP78-1 (from 20 pmol to 80 pmol). The siRNA was administered to 50,000 cells/well in 24 well plates (4 wells/treatment; with duplicate plate). Western blot and Trypan blue exclusion assays were used to determine GRP78 knockdown and HepG2 cell death, respectively. Western blot studies revealed an effect of siRNA treatment on GRP78 protein expression of HepG2 cells 48 hours post treatment led to fifty percent knockdown of GRP78 expression when a concentration of 20 pmol of siRNA, while sixty percent knockdown of GRP78 was observed when 40, 60, and 80 pmol of siRNA were used. Based on the results of the Western blot studies, the optimal siRNA concentration for our studies was 40 pmol (Fig2A).

Forty-eight hours post transfection of siRNA GRP78-1 (20 – 80 pmol) there was less than 5% cell death of HepG2 cells (Fig2C).

To determine the time period for the optimal knockdown of GRP78 expression for RNAi transfection a Western blot study was conducted. Fifty-thousand cells/well were grown in 24 well plates (6 wells/sample; with a duplicate plate) and lysed 24, 72, and 96 hours post transfection of 40 pmol of siRNA GRP78-1 (Fig1D). GRP78 protein levels were measured by Western blot at 24, 48 and 96 hours post transfection. There was no significant difference in levels of GRP78 expression at the different time intervals, so 48 hours was chosen as the optimal time period for further RNAi transfection experiments. Blocking experiments were performed using a peptide sequence identical to the GRP78 peptide antigen used for producing the anti-GRP78 antiserum blocker specific for GRP78 validated the GRP78 antibody specificity (Fig1D).

HepG2 cells transfected with 40 pmol of siRNA GRP78-1 and lysed at 24, 48 and 96 hours post transfection confirmed potent (~60%) GRP78 silencing activity.

A.

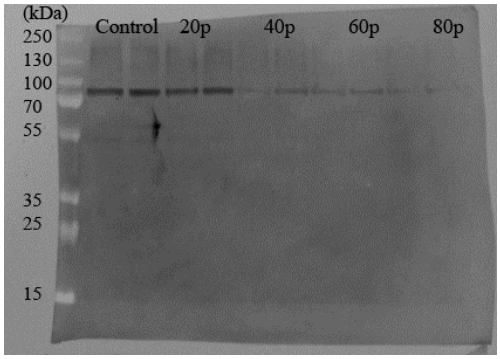

B.

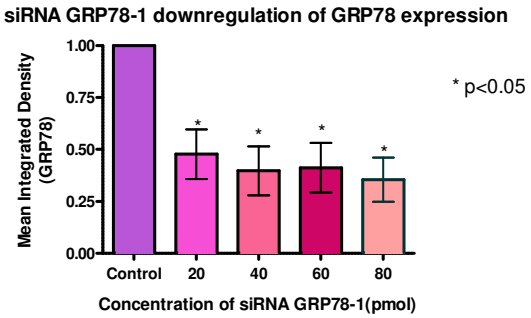

C.

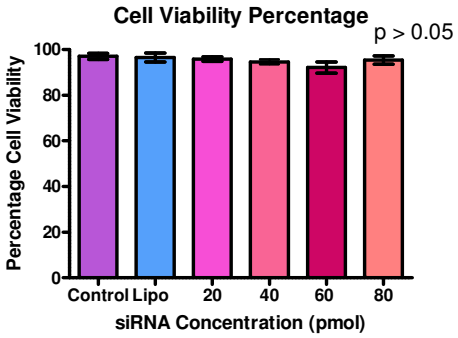

Figure 2: Determining the transfection concentration of a siRNA GRP78-1 construct for HepG2 cells A. Representative western blot is shown (n=5) 50,00 cells/well in 24 well plate transfected with varying concentrations of siRNA GRP78-1; 4 wells per treatment. Fifteen micrograms of protein was loaded per lane. Figure key: lanes 1+2 control, lanes 3+4 20 pmol of siRNA GRP78-1, lanes 5+6 40 pmol, lanes 7+8 60 pmol, lanes 9+10 80 pmol. **B.** GRP78 protein expression levels were established by western blotting and chemiluminescence and quantified using NIH Image J (n=5); statistical significance was determined by ANOVA ($p< 0.05$). **C.** Cell viability percentage values represent the mean +/- S.E.M. Fifty thousand cells/well were plated in 24 well plates. Transfections were carried out with varying amounts of siRNA GRP78-1 and cell viability determined 48 hours post transfection using a Trypan Blue cell exclusion assay. Statistical significance was determined by ANOVA ($p < 0.05$). Figure was modified from Maina et al., 2013.

RNAi of Multiple siRNA Constructs

RNAi transfection experiments of linear, branch, and hyper-branch siRNA specific for GRP78 were conducted within the conditions established in the transfection optimization experiments. Knockdown of GRP78 protein expression was measured by Western blotting analysis 48 hours post transfection (Fig3A). Statistically significant GRP78 expression knockdown was observed with the following constructs: linear GRP78-1 (60%), hyper-branch A-1-2 (58%), V-branch (55%), Y branch and hyper-branch A-1-1 (50%), linear GRP78-2 and linear GRP78-1+GRP78-2 together (40%) (Fig3B).

Trypan blue exclusion assay was conducted 48 hours post transfection and V branch siRNA produced a statistical significant cell death when compared to control and all the other constructs tested (Fig3C). Linear GRP78-1, Linear GRP78-1+GRP78-2 combined had comparable cell viability as control cells. Linear GRP78-2 produced 10% cell death, V branch produced 12% cell death, Y branch and hyper-branch A-1-1 produced 5% cell death, and hyper-branch A-1-2 produced 11% cell death.

A.

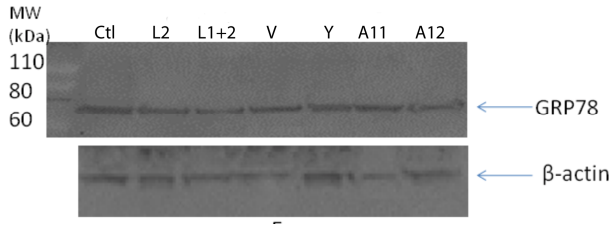

B.

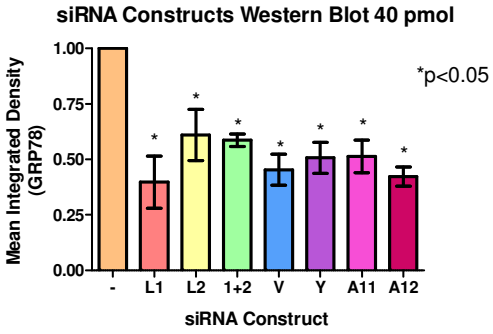

C.

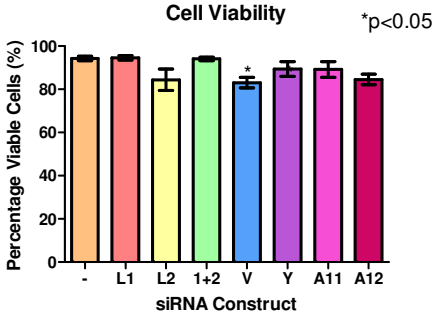

Figure 3: siRNA transfection of HepG2 cells with branch and hyperbranch siRNAs. **A.** Fifty thousand cells/well were plated in 24 well plates with 6 replicate wells per treatment. Forty eight hours post transfection the cells were lysed for immunoblotting and density analysis. Representative blot of three independent experiments. Fifteen micrograms of protein were loaded per lane to determine knockdown level of GRP78 expression, with β-actin serving as a protein loading control. **B.** GRP78 expression levels were quantified using NIH Image J, statistical significant protein knockdown was determined with ANOVA with $p < 0.05$. GRP78 expression level values represent mean +/- S.E.M. for 3 independent experiments. **C.** Cell viability 48 hours post transfection was measured using Trypan blue assay. 50,000 cells/well in 24 well plate; 6 wells/treatment. Cell viability percentage values represent mean +/- S.E. M. for n=4 independent experiments. Statistical significance determined with ANOVA with p value < 0.05. (Figure was modified from Miana et al., 2013)

Confocal Microscopy

Confocal microscopy was conducted 48 hour post treatment of control and transfected HepG2 cells with A-1-2 hyper-branch siRNA to detect GRP78 protein localization and expression levels (Fig4A). Fifty total cells per field for both the control and transfected cells post transfection. There were 15 transfected cells with GRP78 signal compared to 45 control cells 48 hours post transfection (Fig4B). Forty-eight hours post transfection, 32% of A-12 hyper-branch siRNA transfected cells contained GRP78 signal while 93% of control cells contained GRP78 signal (Fig4C).

A.

Control

A-1-2 Hyper-branch siRNA

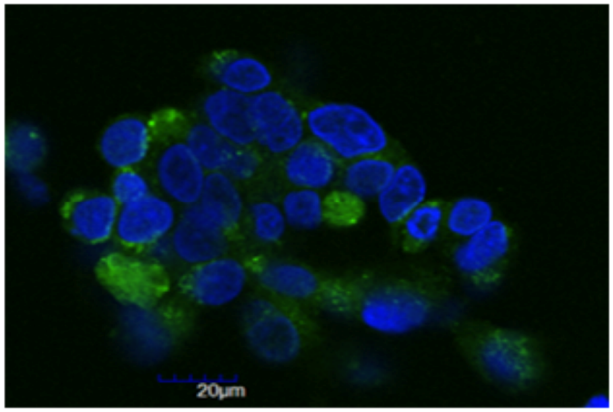

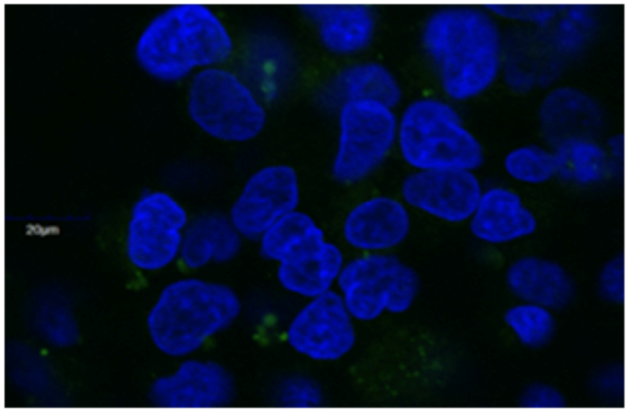

B.

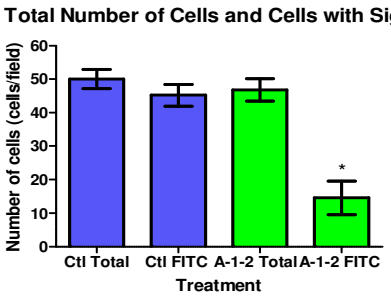

C.

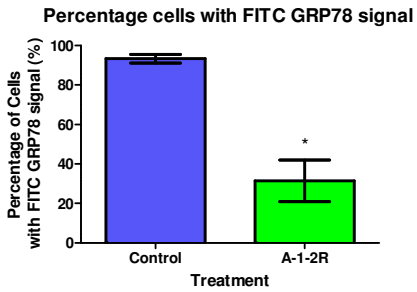

Figure 4: Confocal microscopy of paraformaldehyde fixed HepG2 cells immunostained with an anti-GRP78 antibody (FITC; green) or labeled with DAPI. Cells were viewed using an 40X oil objective lens, and the cells shown are representative of separate viewing fields from five field two independent experiments. **A.** HepG2 cells transfected with A-1-2 Hyper-branch siRNA GRP78. Forty eight hours post transfection cells were fixed with 2 % paraformaldehyde and stained with DAPI (blue), and FITC conjugated to GRP78 protein expression (green). **B.** Mean +/- S.E.M. of the total number of cells/field and the number of cells with FITC signal were counted for both the control and transfected sample. **C.** Percentage of the HepG2 cells with FITC-GRP78 signal for both the control and transfected sample. Statistical significance determined with Student's t-test and p value < 0.05 (Figure modified from Maina et al., 2013).

Table 1: siRNA Sequences

Linear 1a	5′-AGUGUUGGAAGAUUCUGAU-3′	
b	5′-AUCAGAAUCUUCCAACACU-3′	
Linear 2a	5′-GGAGCGCAUUGAUACUAGA-3′	
b	5′-UCUAGUAUCAAUGCGCUCC-3′	
Branched:		
V	2′3′ UCACAACCUUCUAAGACUA-5′ 5′-rU 3′5′ AGUGUUGGAAGAUUCUGAU-3′	
Y	2′3′ UCACAACCUUCUAAGACUA-5′ 5′-UCACAACC-3′5′-rU 3′5′AGUGUUGGAAGAUUCUGAU-3′	
Hyperbranch:		
A-1-1	3′-UAGUCUUAGAGGAUUGUGA-5′2′ rU-3050–UCA CAA CC–3050-rU 5′-AUCAGAAUCUCCUAACACU-3′5′	2′3′ UCACAACCUUCUAAGACUA-5′ 3′5′-AGUGUUGGAAGAUUCUGAU-3′
A-1-2	3′-AGAUCAUAGUUACGCGAGG-5′2′ rU3′5′–UCA CAA CC–3′5′-rU 5′-UCUAGUAUCAAUGCGCUCC-3′	2′3′UCACAACCUUCUAAGACUA-5′ 3′5′ AGUGUUGGAAGAUUCUGAU-3′

Linear sequences 1a 1b, V branch, Y branch, and A-1-1 are derived from nucleotides 1236 – 1255 containing initiation codon for GRP78 mRNA. Linear sequence 2 derived from nucleotides 1887 – 1906 of GRP78 mRNA. A-1-2 Hyperbranch contains sequences derived from a and b. Table modified from Maina et al., 2013

DISCUSSION

Chemotherapy remains a crucial tool in cancer patient therapy. However, despite significant advances in identifying and delineating cancer types, many commonly used chemotherapeutic protocols remain relatively non-selective. By targeting primarily the cancer cell's accelerated growth and metabolic pathways, both normal and cancer cells are subject to chemotherapy treatment toxicity, leading to undesirable side effects. Given these significant limitations, the delivery of highly selective and effective chemotherapy is needed (Hanahan and Weinberg, 2011) to improve cancer patient treatment methods.

To address this unmet medical need research has focused on the cancer cell's unique physiology and protein expression profile. A 2003 proteomic study of cancer cell proteins, revealed the cell surface expression of endoplasmic reticulum (ER) chaperone proteins (Shin et al., 2003). Studies have demonstrated that the endoplasmic reticulum chaperone protein, glucose regulated protein (GRP78) resides on the cancer cell surface (Ni et al., 2011). Importantly, the extracellular exposure of GRP78 is crucial for the progression and metastasis of tumors, and protects the cells from apoptotic programmed cell death (Ni et al., 2011). These distinctive properties make cell surface GRP78 a suitable target for RNA interference technique. A previous study has demonstrated the silencing of GRP78 gene expression by RNA interference suppressed cell survival signaling. A study conducted by Misra in 2006 demonstrated that the binding of alpha-2 macroglobulin to cell surface GRP78 activated the cell survival and proliferation pathways (Misra et al., 2006).

Our studies (Maina et al., 2013) have demonstrated the successful knockdown of GRP78 protein expression in HepG2 cells. We transfected HepG2 cancer cells with multiple GRP78-targeting siRNAs, including: 3 linear, 2 branched, and 2 hyper-branched. The V and Y branched siRNAs contain a single branchpoint nucleotide which combines the sense and antisense strands

within a single molecular structure (Table 1). Hyper-branch siRNAs were designed to contain two siRNA motifs embedded within the same molecular structure by containing multiple branchpoint nucleotides (Maina et al. 2013). The siRNAs target single (linear construct GRP78-1 and GRP78-2) or double sites of GRP78 mRNA expression (A-1-2 hyper-branch siRNAs). The linear sequence GRP78-1, V and Y branched siRNAs were derived from nucleotides 1236-1255 containing the initiation codon for GRP78 mRNA. The linear GRP78-2 siRNA was derived from nucleotides 1887-1906 GRP78 mRNA. A-1-2 hyper-branch contained nucleotides derived from both sequences and serves as a double knockdown siRNA construct (Maina et al., 2013). The linear constructs (siRNA-GRP78-1 and siRNA-GRP78-2) each targeted different, unique GRP78 mRNA sequences. Both of these constructs produced significant GRP78 knockdown (50-60%); an indication that these GRP78 mRNA expression sites are valid targets for inhibiting GRP78 expression. The third linear construct involved combining siRNA-GRP78-1 and siRNA-GRP78-2 together and served as a control against the hyper-branched A-1-2 construct.

All seven constructs produced significant knockdown (40-60%) of GRP78 expression in HepG2 cells ($n=3$; $p<0.05$). The siRNA-GRP78-1 construct and the siRNA-hyper-branch A-1-2 construct produced the greatest knockdown (58 – 60%). Comparison of GRP78 knockdown between A-1-2 hyper-branched siRNA with the linear combination of siRNA-GRP78-1 + GRP78-2 revealed that the A-1-2 hyper-branch produced 18% more knockdown when compared to linear combination of siRNA-GRP78-1 + GRP78-2 (40% for linear GRP78-1 + GRP78-2). These results indicate that while both the hyper-branch A-1-2 construct and the linear combination of siRNA-GRP78-1 + GRP78-2 construct contained the same sequences; when the

sequences are combined within one molecule (as in A-1-2 hyper-branch), a more effective siRNA knockdown of GRP78 expression occurred compared to the separate linear constructs.

Parallel GRP78 expression studies using laser scanning confocal microscopy and indirect immunofluorescence confirmed the effectiveness of the A-1-2 hyper-branched siRNA constructs in reducing HepG2 cells GRP78 expression. Forty eight hours post transfection, the cells treated with siRNA-A-1-2, only ~32% of cells retained GRP78 signal while control cells retained 93% ($p<0.05$; $n=2$) illustrating the potent GRP78 silencing effects of the A-1-2 hyper-branched siRNA. Laser scanning confocal microscopy presents the image in a single plane, so it is not possible to see all of the cells with their complete GRP78 signal in the same field - possibly accounting for the 93% expression observed, rather than the ideal 100% expression. The confocal microscopy results agree with the immunoblotting results, confirming a statistically significant reduction in GRP78 expression. Further confocal studies need to be conducted with the other siRNA constructs to explore their impact on GRP78 cell expression.

While the siRNA-GRP78-1 linear construct significantly reduced GRP78 expression, only 5% cell death was observed, as assessed by a Trypan blue exclusion assay. In comparison, the V branched siRNA and the hyper-branched A-1-2 siRNA produced 11-12% cell death using the same endpoint assay. These results suggest that the more complex siRNAs, in addition to their significant GRP78 knockdown, may also enhance apoptotic cell death, when compared to the corresponding linear constructs. Reduced GRP78 expression does not directly correlate with apoptotic death, both linear and branched siRNAs produced ~60% reduction, but only branched siRNAs impacted cell death, an implication that reducing GRP78 is only part of the picture. Earlier studies have shown that cell surface GRP78 can directly interact with apoptotic pathway

intermediates by blocking caspase activation and inhibiting apoptosis, thus increasing cell survival (Wang et al., 2009). A decrease in cell surface GRP78 could suppress these anti-apoptotic mechanisms by allowing caspase activation, thereby decreasing GRP78-mediated cancer cell survival. Effectively suppressing cell surface GRP78, would selectively allow cancer cell apoptosis while sparing non-cancerous cells.

The large amount of GRP78 detected in the HepG2 cells indicated these cells would be a good model for GRP78 knockdown and resulting apoptosis studies (Figure 1D). Similar GRP78 knockdown effects have been observed with other human cell lines. For example, GRP78 knockdown in fibrosarcoma cells resulted in the regression of tumors (Lee et al., 2006). The human 1-LN prostate cancer cell line was treated with antibodies against the C-terminal domain of GRP78 inhibited MAP Kinase and AKT activation, which are key anti-apoptotic pro-proliferative signaling mechanisms in multiple cancer cells (Misra et al., 2010). The ability to suppress GRP78 interaction with these pathways may compromise cancer cells ability to thrive and provide an effective and selective cancer therapy.

In a recent study, siRNA transfection in melanoma cells caused a down regulation of GRP78 expression which enhanced ER stress and induced chemotherapeutic agents that promoted cell death (Pfaffenbach et al., 2011). Additional studies have detected extracellular GRP78 in the tumor microenvironment and this extracellular GRP78 aids with tumor cell proliferation by the activation of ERK/AKT pathways (Ni et al., 2011). Akt is a serine/threonine kinase that plays a crucial role in cellular survival and proliferation. Akt can enhance cancer cell survival by blocking pro-apoptotic protein function and inactivating target genes that promote apoptosis (Misra et al., 2010). Fast growing tumors have poor vascularization and elevated

glucose metabolism that can lead to severe hypoxia inducing ER stress. ER stress activates the transcription of the GRP78 promoter and cell surface GRP78 expression serves as protection against further ER stress (Fu et al., 2006). This ER stress activated GRP78 supports its role in pro-proliferative and anti-apoptotic signaling (Misra et al., 2010). Down-regulation of cell surface GRP78 may serve as a good method for enhancing apoptosis of cancer cells by decreasing their anti-apoptotic signaling which is enhanced in cancer cells with cell surface GRP78.

GRP78's presence in the tumor microenvironment could be a contributing factor to the cancer cell multifaceted mechanisms of drug resistance (Wang et al., 2009). A 2006 study of 1-LN prostate cancer cells demonstrated that cell surface GRP78 acts as a signaling receptor for NfK-B and Bcl-2 to promote anti-apoptotic signaling (Misra et al., 2006). Cell surface GRP78 may also inhibit the pro-apoptotic pathway by down-regulating an important pro-apoptotic protein such as Bax, which promotes cell survival and proliferation through PI3 Kinase/Akt signaling and ERK 1/2 (Misra et al., 2006). When Bax is not being inhibited, as in the case with cancer cells perhaps by GRP78 – it is able to disrupt the mitochondrial membrane integrity causing the release of a pro-apoptotic signaling protein cytochrome *c*. Cytochrome *c* activates a cascade of caspases to further apoptosis (Hanahan and Weinberg, 2011). Down-regulating GRP78 expression levels, may allow the pro-apoptotic proteins to function normally and allow apoptosis to occur. An siRNA approach which compromises the anti-apoptotic mechanisms of these resistant cancer cells (by reduction in GRP78 cell surface signaling) may be crucial to causing apoptosis in these evasive cancer cells and gives hope to cancer patients using chemotherapeutic drugs.

CONCLUSION

In this study, we explored the implications of GRP78 reduction in promoting HepG2 cell apoptosis. Using RNA interference we demonstrated that multiple siRNA constructs elicit significant reduction in total cellular GRP78 protein expression (40-60%). The linear siRNA-GRP78-1 and hyper-branch siRNA-A-1-2-GRP78 elicited the most knockdown (58-60%). The siRNA-hyper-branched A-1-2 construct produced 18% more knockdown when compared to its linear control (siRNA-GRP78-1 + GRP78-2). Our results clearly show that combining two different siRNAs within one molecule, promotes a more effective GRP78 reduction. Immunofluorescence with laser scanning confocal microscopy studies of cellular GRP78 confirmed the hyper-branch siRNA A-1-2 effectiveness in reducing GRP78 expression levels. The confocal microscopy studies and the immunoblotting results were in agreement, demonstrating a 58% reduction of GRP78 expression levels. The linear siRNA-GRP78-1 elicited 5% cell death while the more complex siRNAs, V branched and A-1-2 hyper-branched were able to produce the most cell death (11 -12%), revealing they may enhance the apoptotic pathway. We conclude that effective suppression of cellular GRP78 promotes cancer cell apoptosis.

LITERATURE CITED

Bumcrot D., Manoharan M., Koteliansky V., Sah D.W. RNAi therapeutics: a potential new class of pharmaceutical drugs. *Nature Chemical Biology* 2: 711 – 719 (2006).

Cunningham J.J., Gatenby R.A., and Brown J.S. Evolutionay dynamics in cancer therapy. *Molecular Pharmacology* 8: 2094 – 2100 (2011).

El-Serag H.B. and Mason A.C. Rising incidence of hepatocellular carcinoma in the United States. *The New England Journal of Medicine.* 340: 745 – 750 (1999).

Fu Y. and Lee A.S. Glucose regulated proteins in cancer progression, drug resistance and immunotherapy. *Cancer Biology & Therapy* 5: 741 – 744 (2006).

Galluzzi L., Aaronson S.A., Abrams J., Alnemri E.S., Andrews D.W., Baehrecke E.H., Bazan N.G., Balgosklonny M.V., Blomgren K., Borner C., Bredesen, D.E., Brenner C., Castedo M., Cidlowski, J.A., Ciechanover A., Cohen G.M., De Laurenzi V., De Maria R., Deshmukh M., Dylancht, B.D., El-Deiry W.S., Flavell R.A., Fulda S., Garrido C., Golstein P., Gougeon M.-L., Green D.R., Gronemeyer H., Hajnoczky G., Hardwick J.M., Hengartner M.O., Ichijo H., Jaattlea M., Kepp O., Kimchi A., Klionsky D.J., Knight R.A., Kornbluth S., Kumar S., Levine B., Lipton S.A., Lugli E., Madeo F., Malorni W., Marine J. CW., Martin S.J., Medema J.P., Mehlen P., Melino G., Moll U.M., Morselli E., Nagata S., Nicholson D.W., Nicotera P., Nunez G., Oren M., Penninger J., Pervaiz S., Peter M.E., Piacentini M., Prehn J. HM., Puthalakath H., Rabinovich G.A., Rizzuto R., Rodrigues C. MP., Rubinsztein D.C., Rudel P., Scorrano L., Simon H-U., Steller H., Tschopp J., Tsujimoto Y., Vandenabeele P., Vitale I., Vousden K.H., Youle R.J., Yuan J., Zhiovotovsky B., and Kroemer G. Guidelines for the use and interpretation of assays for monitoring cell death in higher eukaryotes. *Cell Death Differentiation* 16: 1093 – 1107 (2009).

Grivennikov S.I., Greten F.R., and Karin M. Immunity, inflammation, and cancer. *Cell* 140: 883 – 899 (2010).

Hanahan D. and Weinberg R.A. Hallmarks of cancer: the next generation . *Cell.* 144: 646 – 674 (2011).

Hashimi A. A., Caldwell J., Gonzalez-Gronow M., Pizzo S.V., Aboumrad D., Pozza L., Al-Bayati H., Weitz J.I., Stafford A., Chan H., Kapoor A., Jacobson D.W., Dickhout J.G. and Austin R.C. Binding of anti-GRP78 autoantibodies to cell surface GRP78 increases tissue factor procoaguant activity via the release of calcium from endoplasmic reticulum stores. *Journal of Biological Chemistry* 285: 28912 – 28923 (2010).

Jamora C, Dennert G, and Lee A.S. Inhibition of tumor progression by suppression of stress protein GRP78/BiP induction in fibrosarcoma B/C10ME. *Proceedings National Academy Sciences (*USA) 93: 7690 – 94 (1996).

Javitt N. Hep G2 cells as a resource for metabolic studies: lipoprotien, cholesterol and bile acids. *Federation American Societies Experimental Biology*: 161 – 168 (1990).

Ji J. and Wang X.W. Clinical implications of cancer stem cell biology in hepatocellular carcinoma. *Semin ars Oncology* 39: 461 – 472 (2012).

Kepp O., Galluzzi L., Lipinski M., Yuan J., and Kroemer G. Cell death assays for drug discovery. *Nature Review* 10: 221 – 237 (2011).

Kim, Y.; Lillo, A.M.; Steiniger, S.C.; Liu, Y.; Ballatore, C.; Anichini, A.; Mortarini, R.; Kaufmann, G.F.; Zhou, B.; Felding-Habermann, B.; Janda, K.D. Targeting heat shock proteins on cancer cells: selection, characterization, and cell-penetrating properties of a peptidic GRP78 ligand. *Biochemistry* 45: 9434 – 9444 (2006).

Lee A.S. GRP78 Induction in cancer: therapeutic and prognostic implications. *Cancer Research* 67: 3496 – 3499 (2007).

Liu Y., Steiniger C.J., Kim Y.S., Kaufmann G.F., Felding-Habermann B., and Janda K.D. Mechanistic studies of a peptidic GRP78 ligand for cancer cell-specific drug delivery. *Molecular pharmaceutics* 4: 435 – 447 (2007).

Luo B. and Lee A.S. The critical roles of endoplasmic reticulum chaperones and unfolded protein response in tumorigenesis and anti-cancer therapies. *Oncogene* 32: 1 – 29 (2013).

Maina A., Blackman B.A., Parronchi, C.J., Morozko E., Bender M.E., Blake A.D., and Sabatino D. Solid-phase synthesis, characterization and RNAi activity of branch and hyperbranch siRNAs. *Bioorganic & Medicinal Chemistry Letters* 19: 5270 – 5274 (2013).

Misra U.K. and Pizzo S.V. Ligation of cell surface GRP78 with antibody directed against the COOH-terminal domain of GRP78 suppresses Ras/MAPK and PI 3-kinase/AKT signaling while promoting caspase activation in human prostate cancer cells. *Cancer Biology & Therapy*: 142 – 152 (2010).

Misra U. K., Deedwania R. and Pizzo S. Activation and cross-talk between Akt, NF-kB, and unfolded protein response signaling in 1-LN prostate cancer cells consequent to ligation of cell surface-associated GRP78. *The Journal of Biological Chemistry*: 13694 – 13707 (2006).

Ni M., Zhang, Y. and Lee, A.S. Beyond the endoplasmic reticulum: atypical GRP78 in cell viability, signaling and therpaeutic targeting. *Biochemical Journal* 434: 181 – 188 (2011).

Ouyang L., Shi Z., Zhao S., Wamg F.T., Zhou T.T., Liu B. and Zao J.K. Programmed cell death pathways in cancer: a review of apoptosis, autophagy and programmed necrosis. *Cell Proliferation* 5: 487 – 498 (2012).

Paddison P.J. and Hannon G.J. RNA interference: the new somatic cell genetics? *Cancer Cell* 2: 17 – 23 (2002).

Pfaffenbach, K. T. and Lee A.S. The critical role of GRP78 in psyiological and pathologic stress. *Current Opinion in Cell Biologiy* : 150-156 (2011).

Rasuchert, Nicole, Brandlein, Stephanie, Holzinger, Elisabeth, Muller-Hermelink, Hans-Konrad and Vollmers, H Peter. A new tumor-specific variant of GRP78 as target for antibody based therapy. *Laboratory Investigation* 88: 375 – 386 (2008).

Sakakibara-Konishi J., Oizumi S., Kikuchi J., Kikuchi E., Mizugaki H., Kinoshita I., Dosaka-Akita H., and Nishimura M. Expression of Bim, Noxa, and Puma in non-small cell lung cancer. *BMC Cancer* 12: 286 – 294 (2012).

Shin, B.K., Wang, H., Yim, A.M., La Naour, F., Brichory, F., Ho Jang, J., Zhao, R., Puravs, E., Tra, J., Michael, C.W., Misek, D.E. and Hanash S.M. Global prolifiling of the cell surface proteome of cancer cells uncovers an abundnace of proteins with chaperone function. *The Journal of Biological Chemistry* : 7607 – 7616 (2003).

Tabernero J., Shapiro G.I., LoRusso P.M., Cervantes A., Schwartz G.K., Weiss, G.J., Paz-Ares L., Cho D.C., Infante J.R., Alsina M., Gounder M.M., Falzone R., Harrop J., Seila White A.C., Toudjarska I., Bumcroft D., Meyers R.E., Hinkle G., Svrzikapa N., Huatbarat R.M., Clausen V.A., Cehelsky J., Nochur S.V., Gamba-Valato C., Vaishnaw A.K., Sah D.W.Y., Gollob J.A., and Burris III H.A. First-in-humans trial of an RNA Interference therapeutic targeting VEGF and KSP in cancer patients with liver involvement. *Cancer Discovery* 3: 406 – 417 (2013).

Wang, M., Wey, S. and Zhang, Y., Ye, R. and Lee, A.S. Role of unfolded protein response regulator GRP78/BiP in development, cancer, and neurological disorders. *Antioxidants & Redox Signaling* 9: 2307 – 2316 (2009).

Yoneda Y., Steiniger S.C., Capková K., Mee J.M., Liu, Y., Kaufmann G.F., Janda, K.D. A cell-penetrating peptidic GRP78 ligand for tumor cell-specific prodrug therapy. *Bioorganic & Medicinal Chemistry Letters* 18: 1632 – 1636 (2008).

Zhang Y., Liu R., Ni M., Gill P. and Lee A.S. Cell surface relocation of the endoplasmic reticulum chaperone and unfolded protein response regulator GRP78/BiP. *The Journal of Biological Chemistry* 285: 15065 – 15075 (2010).